# Limits on a Muon Flux from Neutralino Annihilations in the Sun with the IceCube 22-String Detector

R. Abbasi,[24] Y. Abdou,[18] M. Ackermann,[36] J. Adams,[13] M. Ahlers,[28] K. Andeen,[24] J. Auffenberg,[35] X. Bai,[27] M. Baker,[24] S. W. Barwick,[20] R. Bay,[7] J. L. Bazo Alba,[36] K. Beattie,[8] J. J. Beatty,[15,16] S. Bechet,[10] J. K. Becker,[17] K.-H. Becker,[35] M. L. Benabderrahmane,[36] J. Berdermann,[36] P. Berghaus,[24] D. Berley,[14] E. Bernardini,[36] D. Bertrand,[10] D. Z. Besson,[22] M. Bissok,[1] E. Blaufuss,[14] D. J. Boersma,[24] C. Bohm,[30] J. Bolmont,[36] S. Böser,[36] O. Botner,[33] L. Bradley,[32] J. Braun,[24] D. Breder,[35] T. Burgess,[30] T. Castermans,[26] D. Chirkin,[24] B. Christy,[14] J. Clem,[27] S. Cohen,[21] D. F. Cowen,[32,31] M. V. D'Agostino,[7] M. Danninger,[30] C. T. Day,[8] C. De Clercq,[11] L. Demirörs,[21] O. Depaepe,[11] F. Descamps,[18] P. Desiati,[24] G. de Vries-Uiterweerd,[18] T. DeYoung,[32] J. C. Diaz-Velez,[24] J. Dreyer,[17] J. P. Dumm,[24] M. R. Duvoort,[34] W. R. Edwards,[8] R. Ehrlich,[14] J. Eisch,[24] R. W. Ellsworth,[14] O. Engdegård,[33] S. Euler,[1] P. A. Evenson,[27] O. Fadiran,[4] A. R. Fazely,[6] T. Feusels,[18] K. Filimonov,[7] C. Finley,[24] M. M. Foerster,[32] B. D. Fox,[32] A. Franckowiak,[9] R. Franke,[36] T. K. Gaisser,[27] J. Gallagher,[23] R. Ganugapati,[24] L. Gerhardt,[8,7] L. Gladstone,[24] A. Goldschmidt,[8] J. A. Goodman,[14] R. Gozzini,[25] D. Grant,[32] T. Griesel,[25] A. Groß,[13,19] S. Grullon,[24] R. M. Gunasingha,[6] M. Gurtner,[35] C. Ha,[32] A. Hallgren,[33] F. Halzen,[24] K. Han,[13] K. Hanson,[24] Y. Hasegawa,[12] J. Heise,[34] K. Helbing,[35] P. Herquet,[26] S. Hickford,[13] G. C. Hill,[24] K. D. Hoffman,[14] K. Hoshina,[24] D. Hubert,[11] W. Huelsnitz,[14] J.-P. Hülß,[1] P. O. Hulth,[30] K. Hultqvist,[30] S. Hussain,[27] R. L. Imlay,[6] M. Inaba,[12] A. Ishihara,[12] J. Jacobsen,[24] G. S. Japaridze,[4] H. Johansson,[30] J. M. Joseph,[8] K.-H. Kampert,[35] A. Kappes,[24,*] T. Karg,[35] A. Karle,[24] J. L. Kelley,[24] P. Kenny,[22] J. Kiryluk,[8,7] F. Kislat,[36] S. R. Klein,[8,7] S. Klepser,[36] S. Knops,[1] G. Kohnen,[26] H. Kolanoski,[9] L. Köpke,[25] M. Kowalski,[9] T. Kowarik,[25] M. Krasberg,[24] K. Kuehn,[15] T. Kuwabara,[27] M. Labare,[10] S. Lafebre,[32] K. Laihem,[1] H. Landsman,[24] R. Lauer,[36] H. Leich,[36] D. Lennarz,[1] A. Lucke,[9] J. Lundberg,[33] J. Lünemann,[25] J. Madsen,[29] P. Majumdar,[36] R. Maruyama,[24] K. Mase,[12] H. S. Matis,[8] C. P. McParland,[8] K. Meagher,[14] M. Merck,[24] P. Mészáros,[31,32] E. Middell,[36] N. Milke,[17] H. Miyamoto,[12] A. Mohr,[9] T. Montaruli,[24,†] R. Morse,[24] S. M. Movit,[31] K. Münich,[17] R. Nahnhauer,[36] J. W. Nam,[20] P. Nießen,[27] D. R. Nygren,[8,30] S. Odrowski,[19] A. Olivas,[14] M. Olivo,[33] M. Ono,[12] S. Panknin,[9] S. Patton,[8] C. Pérez de los Heros,[33] J. Petrovic,[10] A. Piegsa,[25] D. Pieloth,[36] A. C. Pohl,[33,‡] R. Porrata,[7] N. Potthoff,[35] P. B. Price,[7] M. Prikockis,[32] G. T. Przybylski,[8] K. Rawlins,[3] P. Redl,[14] E. Resconi,[19] W. Rhode,[17] M. Ribordy,[21] A. Rizzo,[11] J. P. Rodrigues,[24] P. Roth,[14] F. Rothmaier,[25] C. Rott,[15] C. Roucelle,[19] D. Rutledge,[32] D. Ryckbosch,[18] H.-G. Sander,[25] S. Sarkar,[28] K. Satalecka,[36] S. Schlenstedt,[36] T. Schmidt,[14] D. Schneider,[24] A. Schukraft,[1] O. Schulz,[19] M. Schunck,[1] D. Seckel,[27] B. Semburg,[35] S. H. Seo,[30] Y. Sestayo,[19] S. Seunarine,[13] A. Silvestri,[20] A. Slipak,[32] G. M. Spiczak,[29] C. Spiering,[36] M. Stamatikos,[15] T. Stanev,[27] G. Stephens,[32] T. Stezelberger,[8] R. G. Stokstad,[8] M. C. Stoufer,[8] S. Stoyanov,[27] E. A. Strahler,[24] T. Straszheim,[14] K.-H. Sulanke,[36] G. W. Sullivan,[14] Q. Swillens,[10] I. Taboada,[5] O. Tarasova,[36] A. Tepe,[35] S. Ter-Antonyan,[6] C. Terranova,[21] S. Tilav,[27] M. Tluczykont,[36] P. A. Toale,[32] D. Tosi,[36] D. Turčan,[14] N. van Eijndhoven,[34] J. Vandenbroucke,[7] A. Van Overloop,[18] B. Voigt,[36] C. Walck,[30] T. Waldenmaier,[9] M. Walter,[36] C. Wendt,[24] S. Westerhoff,[24] N. Whitehorn,[24] C. H. Wiebusch,[1] A. Wiedemann,[17] G. Wikström,[30,§] D. R. Williams,[2] R. Wischnewski,[36] H. Wissing,[1,14] K. Woschnagg,[7] X. W. Xu,[6] G. Yodh,[20] and S. Yoshida[12]

(IceCube Collaboration)

[1]*III Physikalisches Institut, RWTH Aachen University, D-52056 Aachen, Germany*
[2]*Department of Physics and Astronomy, University of Alabama, Tuscaloosa, Alabama 35487, USA*
[3]*Department of Physics and Astronomy, University of Alaska Anchorage, 3211 Providence Drive, Anchorage, Alaska 99508, USA*
[4]*CTSPS, Clark-Atlanta University, Atlanta, Georgia 30314, USA*
[5]*School of Physics and Center for Relativistic Astrophysics, Georgia Institute of Technology, Atlanta, Georgia 30332, USA*
[6]*Department of Physics, Southern University, Baton Rouge, Louisiana 70813, USA*
[7]*Department of Physics, University of California, Berkeley, California 94720, USA*
[8]*Lawrence Berkeley National Laboratory, Berkeley, California 94720, USA*
[9]*Institut für Physik, Humboldt-Universität zu Berlin, D-12489 Berlin, Germany*
[10]*Université Libre de Bruxelles, Science Faculty CP230, B-1050 Brussels, Belgium*
[11]*Vrije Universiteit Brussel, Dienst ELEM, B-1050 Brussels, Belgium*
[12]*Department of Physics, Chiba University, Chiba 263-8522, Japan*
[13]*Department of Physics and Astronomy, University of Canterbury, Private Bag 4800, Christchurch, New Zealand*
[14]*Department of Physics, University of Maryland, College Park, Maryland 20742, USA*

 © 2009 The American Physical Society

[15]Department of Physics and Center for Cosmology and Astro-Particle Physics, The Ohio State University, Columbus, Ohio 43210, USA
[16]Department of Astronomy, The Ohio State University, Columbus, Ohio 43210, USA
[17]Department of Physics, TU Dortmund University, D-44221 Dortmund, Germany
[18]Department of Subatomic and Radiation Physics, University of Gent, B-9000 Gent, Belgium
[19]Max-Planck-Institut für Kernphysik, D-69177 Heidelberg, Germany
[20]Department of Physics and Astronomy, University of California, Irvine, California 92697, USA
[21]Laboratory for High Energy Physics, École Polytechnique Fédérale, CH-1015 Lausanne, Switzerland
[22]Department of Physics and Astronomy, University of Kansas, Lawrence, Kansas 66045, USA
[23]Department of Astronomy, University of Wisconsin, Madison, Wisconsin 53706, USA
[24]Department of Physics, University of Wisconsin, Madison, Wisconsin 53706, USA
[25]Institute of Physics, University of Mainz, Staudinger Weg 7, D-55099 Mainz, Germany
[26]University of Mons-Hainaut, 7000 Mons, Belgium
[27]Bartol Research Institute and Department of Physics and Astronomy, University of Delaware, Newark, Delaware 19716, USA
[28]Department of Physics, University of Oxford, 1 Keble Road, Oxford OX1 3NP, United Kingdom
[29]Department of Physics, University of Wisconsin, River Falls, Wisconsin 54022, USA
[30]Oskar Klein Centre and Department of Physics, Stockholm University, SE-10691 Stockholm, Sweden
[31]Department of Astronomy and Astrophysics, Pennsylvania State University, University Park, Pennsylvania 16802, USA
[32]Department of Physics, Pennsylvania State University, University Park, Pennsylvania 16802, USA
[33]Department of Physics and Astronomy, Uppsala University, Box 516, S-75120 Uppsala, Sweden
[34]Department of Physics and Astronomy, Utrecht University/SRON, NL-3584 CC Utrecht, The Netherlands
[35]Department of Physics, University of Wuppertal, D-42119 Wuppertal, Germany
[36]DESY, D-15735 Zeuthen, Germany

(Received 14 February 2009; revised manuscript received 27 March 2009; published 21 May 2009)

A search for muon neutrinos from neutralino annihilations in the Sun has been performed with the IceCube 22-string neutrino detector using data collected in 104.3 days of live time in 2007. No excess over the expected atmospheric background has been observed. Upper limits have been obtained on the annihilation rate of captured neutralinos in the Sun and converted to limits on the weakly interacting massive particle (WIMP) proton cross sections for WIMP masses in the range 250–5000 GeV. These results are the most stringent limits to date on neutralino annihilation in the Sun.

DOI: 10.1103/PhysRevLett.102.201302 PACS numbers: 95.35.+d, 14.80.Ly, 96.50.S−, 98.70.Sa

Nonbaryonic cold dark matter in the form of weakly interacting massive particles (WIMPs) is one of the most promising solutions to the dark matter problem [1]. The minimal supersymmetric extension of the standard model (MSSM) provides a natural WIMP candidate in the lightest neutralino $\tilde{\chi}_1^0$ [2]. This particle is weakly interacting only and, assuming $R$-parity conservation, is stable and can therefore survive today as a relic from the big bang. A wide range of neutralino masses, $m_{\tilde{\chi}_1^0}$, from 46 GeV [3] to a few tens of TeV [4] is compatible with observations and accelerator-based measurements. Within these bounds it is possible to construct models where the neutralino provides the needed relic dark matter density.

Relic neutralinos in the galactic halo may become gravitationally trapped in the Sun and accumulate in its center, where they can annihilate each other, producing standard model particles. These may decay, creating neutrinos which can escape and reach Earth. The search presented here aims at detecting neutralino annihilations indirectly by observing an excess of such high energy neutrinos from the Sun. Limits on the neutrino flux from the Sun have previously been reported by BAKSAN [5], MACRO [6], Super-Kamiokande [7], and AMANDA [8].

The IceCube detector [9] records Cherenkov light in the ice from relativistic charged particles created in neutrino interactions. In 2007 the detector consisted of an array of 22 vertical strings with 60 digital optical modules (DOMs) each, deployed in the clear Antarctic ice at the South Pole at depths between 1450 and 2450 m below the ice surface. The vertical spacing between DOMs is 17 m and the horizontal distance between strings is 125 m. Each DOM consists of a pressurized glass sphere containing a 25 cm photomultiplier tube (PMT) and a digitizer board. The PMT waveforms are stored when nearest or next-to-nearest DOMs fire within 1 $\mu$s. The trigger selects time windows when eight DOMs produce waveforms within 5 $\mu$s. The reconstructed first photon arrival times are used to determine the muon direction.

The background in the search for neutrinos from the Sun comes from air showers created by cosmic ray interactions in the atmosphere. The showers cause downwards going atmospheric muon events, triggering at several hundred Hz, and atmospheric muon-neutrino events, triggering at a few mHz. When the Sun is below the horizon, the neutrino signal can be distinguished from the atmospheric muon background by selecting events with upward-going reconstructed muon tracks.

The data set used in this analysis consists of $\sim 4.8 \times 10^9$ triggering events taken while the Sun was below the horizon, corresponding to 104.3 days of live time between 01 June and 23 September 2007. The events were processed

through several filters to reduce the content of atmospheric muon events and to enrich the data set in muon-neutrino events. The analysis was performed in a blind manner such that the azimuth of the Sun was not looked at until the selection cuts were finalized.

Events were first required to have at least ten hit DOMs, and the zenith angle of the line-fit [10] first-guess reconstructed track was required to be larger than 70°. Selected events were subjected to log-likelihood (LLH) fitting of muon tracks [10], which uses the probability distribution of the photon arrival times. Cuts were then placed on the zenith angle of this reconstruction ($90° < \theta_{\mathrm{LLH}} < 120°$) and the width of the likelihood optimum ($\sigma_{\mathrm{LLH}} < 10°$), to select upwards going events of good quality. Very loose cuts were placed on several kinematic quantities to remove a small number of outlying events. The final background reduction was then done using support vector machines (SVMs) [11], multivariate learning machines used to classify events as signal-like or backgroundlike. Twelve event observables, that correlated modestly with one another (correlation coefficient $|c| < 0.5$), were used to train two SVMs with six input observables each. The use of two SVMs allowed minimal correlation ($|c| < 0.3$) between the six observables for each SVM. Training was done with simulated signal events, and a set of real data, not used in the analysis, was taken as background. The observables describe the quality of the track reconstructions and the geometry and the time evolution of the hit pattern, most notably through the opening angle between the line-fit and the LLH tracks, $\sigma_{\mathrm{LLH}}$, the mean minimal distance between the LLH track and the hit DOMs, and the number of hit strings. The SVM input distributions for data and simulated backgrounds were generally in good agreement.

Three types of background were simulated: atmospheric muon events from single and coincident air showers were simulated using CORSIKA [12], and atmospheric $\nu_\mu$ events were simulated following the Bartol spectrum [13]. Solar-WIMP signals were simulated with WIMPSIM [14]. Two neutralino annihilation channels, $W^+W^-$ (hard channel) which produces a harder neutrino energy spectrum, and $b\bar{b}$ (soft channel) which gives rise to a softer neutrino energy spectrum, were simulated for five masses $m_{\tilde{\chi}_1^0} = 250$, 500, 1000, 3000, and 5000 GeV. The neutrinos were propagated through the Sun and to the Earth with full flavor oscillation. Absorption in the Sun is important for neutrinos with energies above a few hundred GeV. A muon and a hadronic shower were generated in the ice near the detector. At the vertices the mean energy of simulated signal muons ranges from about 30 GeV to about 150 GeV depending on signal model, see Table I. For the hard channel $\langle E_\mu \rangle$ decreases for $m_{\tilde{\chi}_1^0} > 3$ TeV owing to neutrino absorption in the Sun and secondary neutrino generation. The muon contribution from tau decay was evaluated to be insignificant and tau vertices were therefore neglected. Propagation of muons through the ice was simulated [15], and the Cherenkov light propagation from the muon to the DOMs was performed with [16], taking into account measured ice properties [17].

Figure 1 shows the distributions of the product of the two SVM output values, $Q_1 \times Q_2$. As can be seen in the figure the distribution of simulated background is in good agreement with data. The final event sample was selected by requiring $Q_1 \times Q_2 > 0.1$. This cut increased the signal:$\sqrt{\text{background}}$ ratio by a factor of 8.

Simulations predict that the final data sample of 6946 events has an atmospheric $\nu_\mu$ event content of 56%, and that the remainder consists of misreconstructed atmospheric muon events. The loose cuts maintain a large effective volume, defined as the detector volume with 100% selection efficiency, since the final signal determination was done on the basis of direction.

After calculating the Sun's position, the observed number of events as a function of the angle to the Sun, $\Psi$, is compared to the atmospheric background expectation in Fig. 2. The angular distribution is consistent with the expected background and no excess of events from the Sun is observed.

Using likelihood-ratio hypothesis tests the observed $\Psi$ distribution is fitted with a sum of distributions of the

TABLE I. Upper limits on the number of signal events $\mu_s$, the conversion rate $\Gamma_{\nu\to\mu}$, the neutralino annihilation rate in the Sun $\Gamma_A$, the muon flux $\Phi_\mu$, and the neutralino-proton scattering cross-sections (spin-independent, $\sigma^{\mathrm{SI}}$, and spin-dependent, $\sigma^{\mathrm{SD}}$), at the 90% confidence level including systematic errors. The sensitivity $\bar{\Phi}_\mu$ (see text) is shown for comparison. Also shown is the median angular error $\Theta$, the mean muon energy $\langle E_\mu \rangle$, the effective volume $V_{\mathrm{eff}}$, and the $\nu_\mu$ effective area $A_{\mathrm{eff}}$.

| $m_{\tilde{\chi}_1^0}$ (GeV) | Channel | $\mu_s$ | $\Gamma_{\nu\to\mu}$ ($\mathrm{km^{-3}\,y^{-1}}$) | $\Gamma_A$ ($\mathrm{s^{-1}}$) | $\Phi_\mu$ ($\mathrm{km^{-2}\,y^{-1}}$) | $\bar{\Phi}_\mu$ ($\mathrm{km^{-2}\,y^{-1}}$) | $\sigma^{\mathrm{SI}}$ ($\mathrm{cm^2}$) | $\sigma^{\mathrm{SD}}$ ($\mathrm{cm^2}$) | $\Theta$ | $\langle E_\mu \rangle$ (GeV) | $V_{\mathrm{eff}}$ ($\mathrm{km^3}$) | $A_{\mathrm{eff}}$ ($\mathrm{m^2}$) |
|---|---|---|---|---|---|---|---|---|---|---|---|---|
| 250 | Hard | 7.5 | $3.2 \times 10^3$ | $6.0 \times 10^{21}$ | $8.8 \times 10^2$ | $1.6 \times 10^3$ | $3.7 \times 10^{-43}$ | $2.8 \times 10^{-40}$ | 3.2° | 68.7 | $8.1 \times 10^{-3}$ | $1.3 \times 10^{-4}$ |
| 500 | Soft | 8.5 | $2.8 \times 10^4$ | $1.4 \times 10^{23}$ | $3.5 \times 10^3$ | $5.7 \times 10^3$ | $2.5 \times 10^{-41}$ | $2.6 \times 10^{-38}$ | 3.5° | 28.8 | $1.1 \times 10^{-3}$ | $6.7 \times 10^{-6}$ |
| | Hard | 6.8 | $1.0 \times 10^3$ | $1.6 \times 10^{21}$ | $4.2 \times 10^2$ | $7.9 \times 10^2$ | $2.9 \times 10^{-43}$ | $3.0 \times 10^{-40}$ | 2.9° | 111 | $2.4 \times 10^{-2}$ | $4.9 \times 10^{-4}$ |
| 1000 | Soft | 7.5 | $7.8 \times 10^3$ | $3.0 \times 10^{22}$ | $1.3 \times 10^3$ | $2.4 \times 10^3$ | $1.8 \times 10^{-41}$ | $2.2 \times 10^{-38}$ | 3.2° | 40.8 | $3.4 \times 10^{-3}$ | $2.6 \times 10^{-5}$ |
| | Hard | 6.8 | $6.7 \times 10^2$ | $1.2 \times 10^{21}$ | $3.6 \times 10^2$ | $6.3 \times 10^2$ | $7.2 \times 10^{-43}$ | $8.7 \times 10^{-40}$ | 2.9° | 146 | $3.5 \times 10^{-2}$ | $7.6 \times 10^{-4}$ |
| 3000 | Soft | 7.8 | $3.5 \times 10^3$ | $1.1 \times 10^{22}$ | $7.9 \times 10^2$ | $1.3 \times 10^3$ | $5.3 \times 10^{-41}$ | $7.2 \times 10^{-38}$ | 3.1° | 55.8 | $7.7 \times 10^{-3}$ | $6.9 \times 10^{-5}$ |
| | Hard | 6.4 | $6.1 \times 10^2$ | $1.5 \times 10^{21}$ | $3.3 \times 10^2$ | $6.1 \times 10^2$ | $7.4 \times 10^{-42}$ | $9.9 \times 10^{-39}$ | 2.9° | 149 | $3.7 \times 10^{-2}$ | $7.3 \times 10^{-4}$ |
| 5000 | Soft | 7.5 | $2.8 \times 10^3$ | $8.3 \times 10^{21}$ | $6.7 \times 10^2$ | $1.1 \times 10^3$ | $1.1 \times 10^{-40}$ | $1.5 \times 10^{-37}$ | 3.1° | 59.9 | $9.3 \times 10^{-3}$ | $8.6 \times 10^{-5}$ |
| | Hard | 6.8 | $7.0 \times 10^2$ | $2.0 \times 10^{21}$ | $3.6 \times 10^2$ | $6.6 \times 10^2$ | $2.6 \times 10^{-41}$ | $3.6 \times 10^{-38}$ | 2.9° | 142 | $3.4 \times 10^{-2}$ | $6.2 \times 10^{-4}$ |

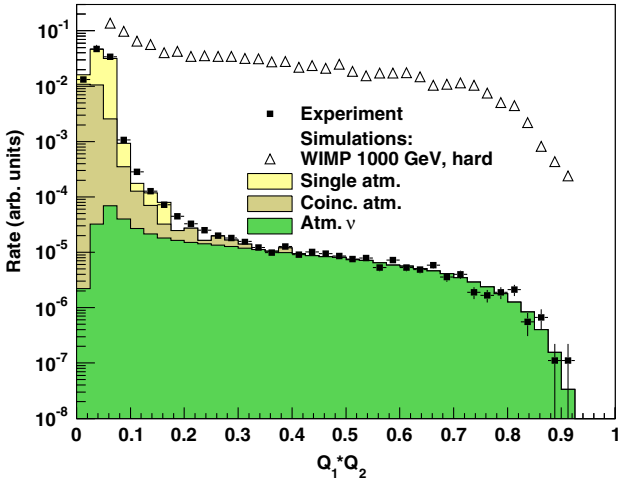



FIG. 1 (color online). The product $Q_1 \times Q_2$ of the output values of the two SVMs for the experimental data, a simulated signal ($m_{\tilde{\chi}_1^0} = 1000$ GeV, hard spectrum) and the background. The background has been scaled to match the data rate and it is shown divided into three components: atmospheric neutrinos and single and coincident atmospheric muons.

simulated signal and the expected background. Here, the expected background is determined by using real data with randomized azimuth direction of the Sun. We then follow the unified Feldman-Cousins approach [18] to construct the confidence intervals on the number of signal events $\mu_s$. The upper 90% confidence limit ranges between $\mu_s = 6.4$ and $\mu_s = 8.5$ events depending on signal case; see Table I.

Simulation studies were used to estimate the systematic uncertainty on the signal effective volume $V_{\text{eff}}$. Uncertainties in the photon propagation in ice and absolute DOM efficiency dominate, contributing $\pm 17\%$ to $\pm 24\%$ depending on the signal model. The total systematic uncertainty on $V_{\text{eff}}$ ranges from $\pm 19\%$ for the highest $m_{\tilde{\chi}_1^0}$ to $\pm 26\%$ for the lowest $m_{\tilde{\chi}_1^0}$. Deviations in the event rate between data and background simulations are within the systematic uncertainty. These uncertainties are included in the results presented below.

From the upper limits on $\mu_s$ we calculate the limit on the neutrino to muon conversion rate $\Gamma_{\nu\to\mu} = \frac{\mu_s(\Psi)}{V_{\text{eff}} t}$, for the live time $t$. Using the signal simulation [14], we can convert this rate to a limit on the neutralino annihilation rate in the Sun, $\Gamma_A$, see Table I. Results from different experiments are commonly compared by calculating the limit on the muon flux above 1 GeV, $\Phi_\mu$, which is also shown in Table I together with the sensitivity, $\bar{\Phi}_\mu$, the median limit obtained from simulations with no signal. A downward fluctuation in the data close to the position of the Sun results in limits lower than the sensitivity. Within $\Psi < 3°$, corresponding to the rightmost bin in Fig. 2, the fluctuation has a probability of 8.8%. In this bin we expect less than 0.4 background events from solar atmospheric neutrinos [19].

The 90% confidence upper limit on $\Phi_\mu$ as a function of $m_{\tilde{\chi}_1^0}$ is shown in Fig. 3, compared to other limits [6–8], and MSSM model predictions [20]. In the plot, the shaded area represents neutralino models not disfavored by the direct detection experiments CDMS [21] and XENON-10 [22], based on their limit on the spin-independent neutralino-proton cross section.

The limits on the annihilation rate can be converted into limits on the spin-dependent, $\sigma^{\text{SD}}$, and spin-independent,

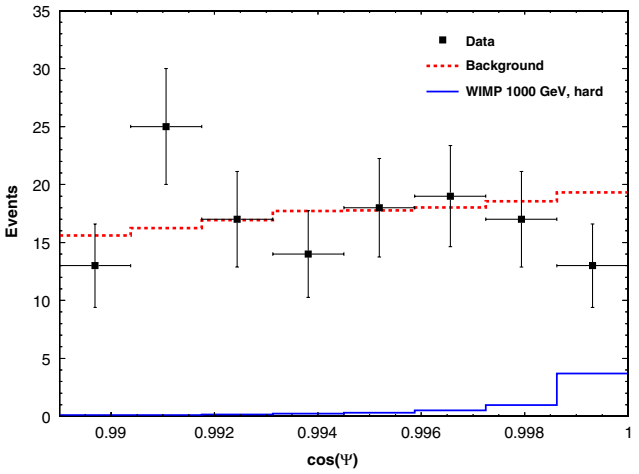



FIG. 2 (color online). Cosine of the angle between the reconstructed track and the direction of the Sun, $\Psi$, for data (squares) with 1 standard deviation error bars, and the atmospheric background expectation from atmospheric muons and neutrinos (dashed line). Also shown is a simulated signal ($m_{\tilde{\chi}_1^0} = 1000$ GeV, hard spectrum) scaled to $\mu_s = 6.8$ events (see Table I).

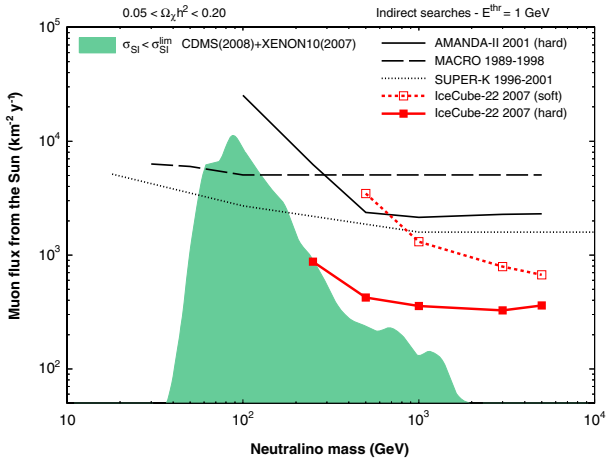



FIG. 3 (color online). Upper limits at the 90% confidence level on the muon flux from neutralino annihilations in the Sun for the soft ($b\bar{b}$) and hard ($W^+W^-$) annihilation channels, adjusted for systematic effects, as a function of neutralino mass. The shaded area represents MSSM models not disfavored by direct searches [21,22]. A muon energy threshold of 1 GeV was used when calculating the flux. Also shown are the limits from MACRO [6], Super-K [7], and AMANDA [8].

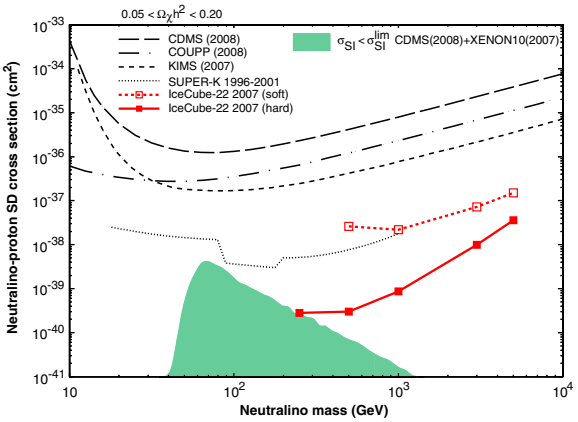



FIG. 4 (color online). Upper limits at the 90% confidence level on the spin-dependent neutralino-proton cross section $\sigma^{\mathrm{SD}}$ for the soft ($b\bar{b}$) and hard ($W^+W^-$) annihilation channels, adjusted for systematic effects, as a function of neutralino mass. The shaded area represents MSSM models not disfavored by direct searches [21,22] based on $\sigma^{\mathrm{SI}}$. Also shown are the limits from CDMS [21], COUPP [25], KIMS [24], and Super-K [7].

$\sigma^{\mathrm{SI}}$, neutralino-proton cross sections, allowing a more direct comparison with the results of direct search experiments. Since capture in the Sun is dominated by $\sigma^{\mathrm{SD}}$, indirect searches are expected to be competitive in setting limits on this quantity. Assuming equilibrium between the capture and annihilation rates in the Sun, the annihilation rate is directly proportional to the cross section. A limit on $\sigma^{\mathrm{SD}}$ is found by setting $\sigma^{\mathrm{SI}}$ to zero, and vice versa. We have used DARKSUSY [20] and the method described in [23] to perform the conversion. The results are shown in Table I. We assumed a local WIMP density of 0.3 GeV/cm$^3$, and a Maxwellian WIMP velocity distribution with a dispersion of 270 km/s. Planetary effects on the capture were neglected. Figure 4 shows the IceCube-22 limits on $\sigma^{\mathrm{SD}}$ compared with other bounds [7,21,24,25], and the MSSM model space defined as for Fig. 3. Indirect searches for dark matter in the Sun complement direct searches on Earth in several respects. WIMPs in the Sun would accumulate over a long period and therefore sample over different dark matter densities in the galactic halo. This gravitational accumulation is sensitive to low WIMP velocities while direct detection recoil experiments are more sensitive at higher velocities.

In conclusion, we have presented the most stringent limits to date on neutralino annihilations in the Sun, improving on the 2001 AMANDA [8] limits by at least a factor of 6 for hard channels. We also present the most stringent limits on the spin-dependent WIMP-proton cross section for neutralino masses above 250 GeV. The full IceCube detector with the DeepCore extension [26] is expected to test viable MSSM models down to 50 GeV.

We acknowledge support from the following agencies: U.S. National Science Foundation-Office of Polar Programs, U.S. National Science Foundation-Physics Division, U. of Wisconsin Alumni Research Foundation, U.S. Department of Energy, NERSC, the LONI grid; Swedish Research Council, K. & A. Wallenberg Foundation, Sweden; German Ministry for Education and Research, Deutsche Forschungsgemeinschaft; Fund for Scientific Research, IWT-Flanders, BELSPO, Belgium; the Netherlands Organisation for Scientific Research; M. Ribordy is supported by SNF (Switzerland); A. Kappes and A. Groß are supported by the EU Marie Curie OIF Program. We thank J. Edsjö for DARKSUSY support.

*Present address: Universität Erlangen-Nürnberg, Physikalisches Institut, D-91058, Erlangen, Germany.
†On leave from Università di Bari and Sezione INFN, Dipartimento di Fisica, I-70126, Bari, Italy.
‡Present address: School of Pure and Applied Natural Sciences, Kalmar University, S-39182 Kalmar, Sweden.
§Corresponding author.
wikstrom@physto.se

[1] V. Rubin and W. K. Ford, Astrophys. J. **159**, 379 (1970).
[2] M. Drees and M. M. Nojiri, Phys. Rev. D **47**, 376 (1993).
[3] C. Amsler *et al.*, Phys. Lett. B **667**, 1 (2008).
[4] R. C. Gilmore, Phys. Rev. D **76**, 043520 (2007).
[5] M. M. Boliev *et al.*, Nucl. Phys. B, Proc. Suppl. **48**, 83 (1996).
[6] M. Ambrosio *et al.*, Phys. Rev. D **60**, 082002 (1999).
[7] S. Desai *et al.*, Phys. Rev. D **70**, 083523 (2004).
[8] M. Ackermann *et al.*, Astropart. Phys. **24**, 459 (2006).
[9] A. Achterberg *et al.*, Astropart. Phys. **26**, 155 (2006).
[10] J. Ahrens *et al.*, Nucl. Instrum. Methods Phys. Res., Sect. A **524**, 169 (2004).
[11] S. S. Kerthi *et al.*, Neural Comput. **13**, 637 (2001).
[12] D. Heck *et al.*, FZKA Report No. 6019, 1998.
[13] G. D. Barr *et al.*, Phys. Rev. D **70**, 023006 (2004).
[14] M. Blennow, J. Edsjö, T. Ohlsson, J. Cosmol. Astropart. Phys. 01 (2008) 021.
[15] D. Chirkin and W. Rhode, arXiv:hep-ph/0407075v2.
[16] J. Lundberg *et al.*, Nucl. Instrum. Methods Phys. Res., Sect. A **581**, 619 (2007).
[17] M. Ackermann *et al.*, J. Geophys. Res. **111**, D13203 (2006).
[18] G. J. Feldman and R. D. Cousins, Phys. Rev. D **57**, 3873 (1998).
[19] G. Ingelman and M. Thunman, Phys. Rev. D **54**, 4385 (1996).
[20] P. Gondolo *et al.*, J. Cosmol. Astropart. Phys. 07 (2004) 008.
[21] Z. Ahmed *et al.*, Phys. Rev. Lett. **102**, 011301 (2009).
[22] J. Angle *et al.*, Phys. Rev. Lett. **100**, 021303 (2008).
[23] G. Wikström and J. Edsjö, J. Cosmol. Astropart. Phys. 04 (2009) 009.
[24] H. S. Lee *et al.*, Phys. Rev. Lett. **99**, 091301 (2007).
[25] E. Behnke *et al.*, Science **319**, 933 (2008).
[26] E. Resconi (IceCube Collaboration), Nucl. Instrum. Methods Phys. Res., Sect. A **602**, 7 (2009).